Probing Dynamic Heterogeneity and Amorphous Order Using Rotational Dynamics of Rodlike Particles in Supercooled Liquids

Anoop Mutneja[*] and Smarajit Karmakar[†]

Tata Institute of Fundamental Research, 36/P, Gopanpally Village, Serilingampally Mandal, Ranga Reddy District, Hyderabad, Telangana 500107, India

Probing dynamic and static correlations in glass-forming supercooled liquids has been a challenge for decades despite extensive research. Dynamic correlation, which manifests itself as dynamic heterogeneity, is ubiquitous in various systems starting from molecular glass-forming liquids, dense colloidal systems to collections of cells. On the other hand, the mere concept of growing many-body static correlations in these dense disordered systems in the supercooled regime remains somewhat elusive. Its existence is still actively debated. We propose a method to extract dynamic and static correlations using rodlike particles as a probe. This method can be implemented in experiments to study the growth of static and dynamic correlations in molecular glass-forming liquids and other soft-matter systems, including biological systems that show glassy dynamics. Finally, we analytically derive the exact form of the distribution of rotational decorrelation time of the probe rod molecules and rationalize the observed log-normal-like distribution reported in previous experimental studies on the dynamics of elongated probe molecules in supercooled glycerol.

I. INTRODUCTION

Being structurally disordered, constituent particles or molecules in both the liquid and glass phases experience variable local environments. This can be easily ignored for high-temperature liquids, but for supercooled liquids, it manifests itself in the spatial distribution of particle's mobility, from nearly stuck to fairly moving. This, in turn, gives rise to complex behavior in their bulk properties like viscosity, structural relaxation time, and diffusion constant. These complex dynamical behaviors are termed in the literature as dynamical heterogeneity (DH) [1,2]. The slow- and fast-moving local regions form clusters [3–5], which lead to substantial spatial variation in the system's local relaxation times.

On the other hand, the absence of any causal link [6–8] between the growing dynamical heterogeneity length scale, ξ_D, and the increasing relaxation time, τ_α (defined in the Supplemental Material [9]) or the viscosity, suggests the existence of yet another length scale. In Ref. [6], it was proposed that a static length scale, ξ_S, also grows with decreasing temperature, and its existence is consistent with the predictions of random first-order transition (RFOT) theory [10,11]. In Ref. [12], a correlation function, known

as point-to-set (PTS) correlation function (see the Supplemental Material [9] for a definition), was proposed and estimated in various model glass-forming liquids to extract ξ_S, which is found to be causally related to τ_α. Various other measures of ξ_S are also found to be consistent with each other [13,14]. The underlying structural order related to the PTS length scale is often referred to as "amorphous order." It is now broadly believed that two different length scales probably grow while approaching glass transition [15,16]. However, a possible mutual relation between these two length scales remains poorly understood [17].

The ξ_D is computed in general using χ_4^P, the peak value of four-point susceptibility $\chi_4(t)$ [18,19] (see the Supplemental Material [9] for a definition), which is assumed to be related to ξ_D as $\chi_4^P \sim \xi_D^{2-\eta}$ with η being an unknown exponent. ξ_D can also be computed from the spatial correlation in the particle's mobility field [20–22]. Recently, in Ref. [23,24], the non-Gaussian nature of the van Hove function is used to probe ξ_D very efficiently by systematic coarse graining (block analysis) the system at varying length scales. The idea is that upon coarse graining over the length scale comparable or larger than ξ_D, one would expect that the van Hove function will tend to become Gaussian. This work shows how dynamics of rodlike particles in supercooled liquids with varying rod lengths similarly probe the system's response at varying coarse-graining length scales and thereby similarly extract ξ_D.

---

[*]anoopmutneja@tifrh.res.in
[†]smarajit@tifrh.res.in

Although the direct experimental measurements of χ_4 or displacement-displacement correlation function are conceivable for colloidal or granular systems [25–29], it is impossible to do so for molecular liquids as complete spatial and temporal resolution of the trajectories of all particles in a system is needed. Thus for molecular liquids, one often measures $\chi_4(t)$ indirectly, as shown in Ref. [30]. Nevertheless, an accurate estimate of the length scale will still not be possible as the exponent, η, is *a priori* unknown [31–33]. Similarly, an experimental measure of growing amorphous order is also minimal, and direct evidence of a growing ξ_S came from the measurement of fifth-order dielectric susceptibility [$\chi_5(t)$] [34] and via random pinning using holographic optical tweezers [35]. The experimental measurements' intricacy immediately tells us that an accurate estimation of growing amorphous order is still tricky. Thus the strong experimental evidence of the growth of both ξ_D and ξ_S in molecular glass-forming liquids is still lacking. A simple experimentally realizable proposal for possible measurements of these two length scales will definitely be useful for understanding the glass transition puzzle.

In particular, the experiments on the rotational dynamics of single-molecule (SM) probes using various techniques [36–42] are very encouraging. In these SM experiments, on lowering the temperature, the link to increased dynamic heterogeneity is made via the increase in width of the distribution of rotational correlation time or observed decorrelation of translation and rotational dynamics. The decorrelation-time distribution is observed to be log normal. Simultaneously, the switch from Debye diffusion (small random steps) to large, infrequent rotational hops with decreasing temperature has been linked with the underlying structural relaxation time. The infrequent α relaxation of local particles would make the probe hop and explain the switch [43–45], but a direct measure of ξ_D and ξ_S will still be unavailable. Here, we propose that the SM probe experiments can measure the growth of both ξ_D and ξ_S, if the probe molecule's length is varied while studying their rotational dynamics. These experiments are feasible with the available probes for various glass-forming liquids [36–41].

II. MODELS AND METHODS

This work contains extensive simulations of three model glass-forming liquids, namely (i) the three-dimensional Kob-Andersen binary Lennard-Jones mixture (3DKA)[46], (ii) a similar model in two dimensions (2DMKA) [47], and (iii) the three-dimensional binary mixture of particles interacting via harmonic potential (3DHP) [48]. The units of length, energy, and time are, respectively, the diameter of the larger particle (σ), the prefactor of the potential energy function (ϵ), and ($\sqrt{m\sigma^2/\epsilon}$) where m is the mass of a particle. The other reduced units can

be derived from these. The usual leap-frog integrator integrates the equation of motion for translational dynamics of spheres and the center of mass of rods. The dynamics of the rod's orientation vector ($\hat{\mathbf{u}}$) is also integrated by the same integrator but strictly following the methods illustrated in Refs. [49,50]. The other details of the models, an example for unit conversion to the real system, and the techniques used in performing *NPT* molecular dynamics simulations with few rodlike particles can be found within the Supplemental Material [9]. The error bars are computed using the optimization method as detailed within the Supplemental Material [9]. The rest of the paper is broadly divided into two parts. In the first part, we discuss the scaling analysis performed to extract ξ_D from the rod-length dependence of the rotational non-normal parameter. Then, we discuss the first-passage-time (FPT) (defined later) distribution of the rod molecules and how one can extract ξ_S from that.

III. NON-NORMAL PARAMETERS AND DYNAMIC HETEROGENEITY LENGTH

We study the rotational dynamics of rodlike probe molecules as done in experiments [36–42] but looked at the changes with varying lengths of the rods as shown in Fig. 1(a). (See the Supplemental Material for other dynamical characterizations of the rod [9].) To quantify the heterogeneity in dynamics, we use the non-normal parameter, α_{2D}, and α_{3D}, for the rods' rotational diffusion. This is similar to the Binder cumulant or the non-Gaussian parameter usually studied in the context of studying dynamic heterogeneity in systems with spherical particles. In Ref. [51], it has been analytically shown that the following will be the appropriate non-normal parameters for distributions $P_{2D}(\phi, t)$ and $P_{3D}(\theta, t)$, where $\phi(t) \in [-\pi, \pi]$ is the polar angle in the 2D system and $\theta(t) \in [0, \pi]$ is the azimuthal angle in the 3D system [assuming the rods are initially placed along the positive x axis in 2D ($\phi = 0$) and along positive z axis ($\theta = 0$) in 3D]

$$\alpha_{2D} = \frac{1}{3} \frac{\left\langle |\hat{u}(t) - \hat{u}(0)|^4 \right\rangle}{\left(\left\langle |\hat{u}(t) - \hat{u}(0)|^2 \right\rangle \right)^2} - \frac{1}{24} \left\langle |\hat{u}(t) - \hat{u}(0)|^2 \right\rangle$$
$$\times \left(\left\langle |\hat{u}(t) - \hat{u}(0)|^2 \right\rangle - 8 \right) - 1, \quad (1)$$

$$\alpha_{3D} = \frac{1}{2} \frac{\left\langle |\hat{u}(t) - \hat{u}(0)|^4 \right\rangle}{\left(\left\langle |\hat{u}(t) - \hat{u}(0)|^2 \right\rangle \right)^2} + \frac{1}{6} \left\langle |\hat{u}(t) - \hat{u}(0)|^2 \right\rangle - 1. \quad (2)$$

Here, $\hat{u}(t)$ is the rod's orientation unit vector at a time "t." At high temperature (or low density), one expects $\alpha_{2D}(t, T)$ or $\alpha_{3D}(t, T)$ to remain small for all rod lengths and at all times. However, for supercooled liquid in the presence of dynamic heterogeneity, one sees a maximum at time scale around $t = \tau_\alpha$ similar to $\chi_4(t, T)$ [Fig. 1(b)]. One also sees that its peak value (α_{2D}^P and α_{3D}^P) grows with decreasing temperature, consistent with the growth of heterogeneity
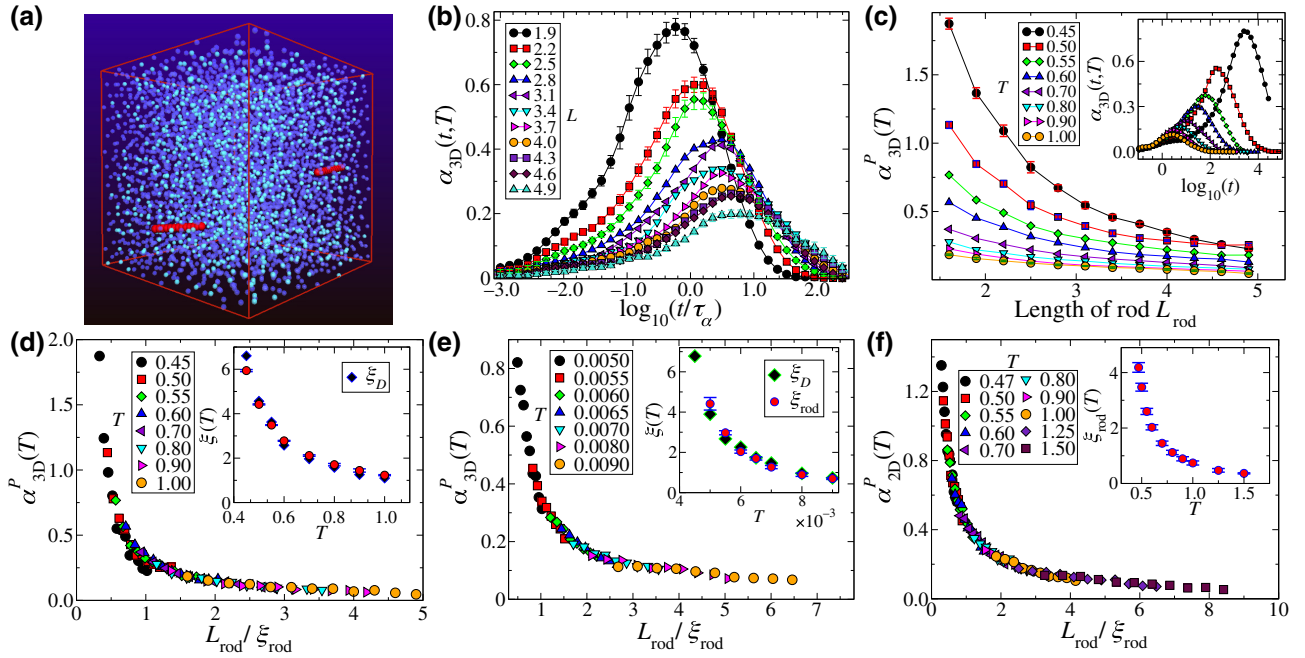
FIG. 1.   (a) Schematic representation of rod particles in the supercooled liquid medium. (b) Evolution of non-normal parameter $[\alpha_{3D}(t, T)]$ for different rod lengths in the 3DKA model at temperature $T = 0.50$. Inset of (c): evolution of $\alpha_{3D}(t)$ for rods of length $L_{rod} = 2.5$ in the same supercooled liquid model at different temperatures. (c) Variation in peak value of α_{3D}^{P} with rod length in the 3DKA system at different supercooling temperatures. Bottom panels: collapse of α_{2D}^{P} or α_{3D}^{P} obtained by scaling the rod length with appropriate correlation length scale ξ_{rod} for all three systems [3DKA, 3DHP, and 2DMKA from (d) to (f)]. In these plots' insets, the scaling length scale is compared with ξ_{D} of the parent liquid obtained by FSS of χ_{4}^{P} [24]. Both the length scales are found to be in good agreement with each other.

in the system [Fig. 1(c), inset]. It is somewhat intuitive to understand the values of α_{2D}^{P} and α_{3D}^{P} will decrease with increasing rod length. The rod will now experience the collective dynamical response of the surrounding liquid medium averaged over a volume of a linear size comparable to the rod's length [Figs. 1(b) and 1(c)]. The top panels of Fig. 1 are for the 3DKA model. The results for other models are very similar and are shown in the Supplemental Material [9]. The error bars in all figures represent ±1 standard error of the mean. Error bars are not shown when they are smaller than the symbol size.

We now discuss a scaling theory that rationalizes the observed rod-length dependence of the non-normal parameters as a function of temperature. If a length scale, ξ_{rod} governs the physics, then one would expect a master plot between α_{3D}^{P} or α_{2D}^{P} and $L_{rod}/\xi_{rod}(T)$, where L_{rod} is the length of the rod. The growth of this length scale $[\xi_{rod}(T)]$ would represent the growing dynamic correlations in the medium with increasing supercooling. Figure 1 (bottom panel) shows the master curves for the 3DKA, 3DHP, and 2DMKA models (left to right). $\xi_{rod}(T)$ are obtained as a fitting parameter to obtain the data collapse (see the Supplemental Material [9] for details). In the insets of Fig. 1 (bottom panel), ξ_{rod} is plotted along with ξ_{D} obtained by Refs. [7,8,24]. The collapse obtained for all of the models

are good, and the obtained length scale matches remarkably well with the dynamic length scale of the system, ξ_{D} obtained using other methods. This gives us the confidence that rodlike molecules can indeed be an excellent probe of the dynamical heterogeneity in glass-forming liquids.

IV. FIRST-PASSAGE-TIME DISTRIBUTION AND STATIC LENGTH SCALE

To understand the observed log-normal decorrelation time distribution of probe molecules in experiments [39,42], we look at the "first-passage-time (FPT)" distribution of rodlike particles in our simulations. The distribution turns out similar but not mathematically identical to log normal (see the Supplemental Material [9] for further details). Note that the decorrelation time distribution is the same as FPT distribution with a chosen cutoff in angular displacement. The FPT distribution, $F(t, \phi_c)$ in 2D, is defined as the probability of rod crossing the angle $\phi = \phi_c$ at a time t for the first time. For the unfolded ϕ coordinate, i.e., $\phi \in (-\infty + \infty)$, this distribution will be the same as that of the FPT distribution of the one-dimensional Brownian particle, i.e., $F(t, x_c) = (x_c/\sqrt{4\pi D_r t^3})e^{-x_c^2/4D_r t}$. Nevertheless, the quantity of interest here would be the distribution of decorrelation time, i.e., $F(t, \pm\phi_c)$. This $F(t, \pm\phi_c)$ is

exactly the distribution of time taken for a one-dimensional Brownian particle to leave the bounded region $[-\phi_c, +\phi_c]$, while starting from $\phi = 0$. For Brownian motion of the rod in 2D, one can easily verify that

$$\mathscr{P}_c(\phi, t) = \frac{1}{\phi_c} \sum_{n=0}^{\infty} \cos\left(\frac{(2n+1)\pi\phi}{2\phi_c}\right) e^{-\frac{(2n+1)^2\pi^2}{4\phi_c^2}Dt} \quad (3)$$

satisfies the rotational diffusion equation with two absorbing boundaries at $\phi = \pm\phi_c$. In this solution, each eigenstate decays exponentially in time with a decay rate of $[(2n+1)^2\pi^2/4\phi_c^2]$. Thus at large times, only the $n = 0$ term would contribute to the survival probability

$$S(t) \propto e^{-\frac{D\pi^2}{4\phi_c^2}t} = e^{-t/\tau}. \quad (4)$$

Thus the first passage time (time derivative of survival probability) will also decay exponentially at long time. Also, one can obtain the following solution for $\mathscr{P}_c(\phi, t)$ by the method of images:

$$\mathscr{P}_c(\phi, t) = \frac{1}{\sqrt{4\pi Dt}} \sum_{n=-\infty}^{\infty} (-1)^n e^{-\frac{(\phi+2n\phi_c)^2}{4Dt}}. \quad (5)$$

Note that the two solutions, Eqs. (3) and (5) are the same but represented via two different series. Readers are encouraged to read Ref. [52] for details. In the limit of short time, only the $n = 0$ term would contribute, leading us to the following expression of survival probability at short times

$$S(t \to 0) \propto \frac{\sqrt{4\pi Dt}}{\sqrt{4\pi Dt}} \text{erf}\left(\phi_c\sqrt{4Dt}\right). \quad (6)$$

Differentiating this survival probability with a negative sign gives us the first-passage-time distribution at short times:

$$F(t \to 0, \pm\phi_c) \propto \frac{\phi_c}{\sqrt{4\pi Dt^3}} e^{-x_c^2/4Dt}. \quad (7)$$

Thus the approximate closed form for the distribution, $F(t, \pm\phi_c)$ and the exact series solution followed from Eq. (3) are given by the following expressions:

$$F(t, \pm\phi_c) \propto t^{-\beta} e^{-\alpha/t} e^{-t/\tau}, \quad (8)$$

$$F(t, \pm\phi_c) = \frac{\pi D}{\phi_c^2} \sum_{n=0}^{\infty} (-1)^n (2n+1) e^{-\frac{(2n+1)^2\pi^2Dt}{(4\phi_c^2)}}. \quad (9)$$

With this exact solution, we can obtain the mean FPT to be $\langle t \rangle = \phi_c^2/2D_r$ and observe that the distribution $P[y = \ln(D_r t)]$ is independent of D where t is the FPT. This

implies that the distribution $P\{y = \ln[t/I(L_{\text{rod}})]\}$ is independent of rod length, with $I(L_{\text{rod}})$ being the moment of the inertia rod of the rod [since $D(L_{\text{rod}}) \sim 1/I(L_{\text{rod}})$ as shown in the Supplemental Material [9] and Ref. [53]]. So we can subtract out this obvious rod-length scaling to understand the effect of supercooled liquid environment on the FPT distributions at various length scales. It is also worthwhile to point out that except for the first moment (mean), no other moment changes for the distribution $P(y = \ln[t])$.

The functional fit using Eq. (8) for the FPT distribution of the Brownian rod with two absorbing boundaries and exact solution Eq. (9) is very good, as shown in the
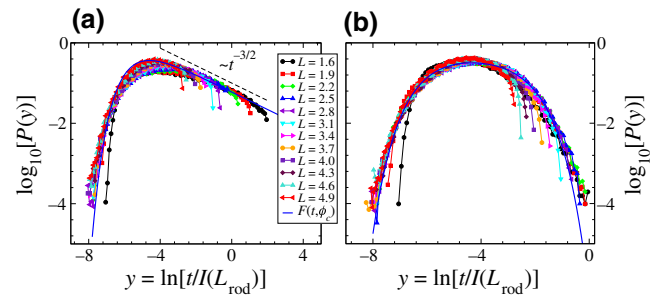

FIG. 2. (a) Distribution of FPT for rods of various lengths scaled by the moment of inertia [$I(L_{\text{rod}})$] in the 2DMKA system at temperature $T = 1.5$ (high temperature) with one absorbing boundary at $\phi_c = \pi/8$. Note that we use unbounded coordinates for this calculation, i.e., $\phi \in [-\infty, +\infty]$. (b) The same distribution with two absorbing boundaries at $\phi = \pm\phi_c$. The bold line is fit to Eq. (8).
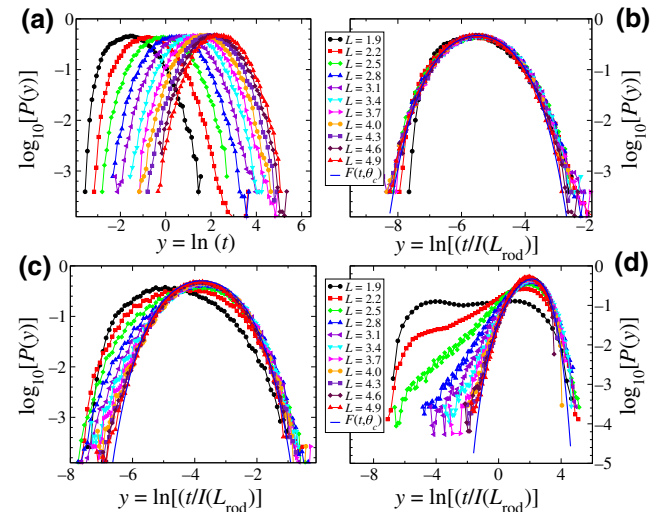

FIG. 3. (a) Distribution of unscaled and (b) scaled FPT (scaled with moment of inertia) for rods of various lengths in 3DKA system at temperature $T = 2.0$ (high temperature) with absorbing boundary at $\theta_c = \pi/8$. Similar scaled distributions at temperature $T = 1.0$ and $T = 0.5$ (low temperatures) with the same boundary conditions are shown in (c),(d). Solid lines are fit to Eq. (8).

Supplemental Material [9]. The value of exponent β comes out to be $\beta = -0.5$ for 2D and $\beta = -1.0$ for 3D (the 3D case is discussed later) along with exponential decay. In Fig. 2, FPT distributions of rods in the 2DMKA system scaled with their moment of inertia $[I(L_{rod})]$ are shown. Long time behavior in Fig. 2 left panel fits very well with $t^{-3/2}$ as expected for a single absorbing boundary, while for two absorbing boundaries, the fitting of Eq. (8) in the right panel of Fig. 2 is also good (deviating only at extreme tail).

Unlike in the 2D case, the FPT distribution in 3D is solved numerically. $F(t, \theta_c)$ in 3D is defined as the probability that the rod crosses the angle $\theta = \cos^{-1}[\hat{u}(t)\hat{u}(0)] = \theta_c$ at time t for the first time. Equation (8) will also describe the FPT distribution of the rod in 3D; arguments leading to that are given in Supplemental Material [9]. Figure 3 top left and right panels are the respective unscaled and scaled FPT distributions of rods embedded in the 3DKA model system at high temperature. One sees similar results for the 3DHP model and is presented in the Supplemental Material [9].

Interestingly, at low temperatures, these FPT distributions develop a shoulder at short times for smaller rods and eventually converge to the same asymptotic distribution for larger rods (Fig. 3 bottom panels). This is the crossover from small-step Debye diffusion to infrequent large-step hopping motions. These results can be rationalized if we assume that the whole system comprises many domains of different mobilities as envisaged in RFOT theory as "mosaic" picture of the supercooled liquid state. Since a smaller size rod can partially fit in one or two such patches, it can have larger instantaneous torques resulting from structural relaxation of these patches and thus hoping. In contrast, a larger rod would span many such patches, thus showing bulklike homogeneous behavior. The skewness of the distribution, $P[\ln(t), \pm \phi_c]$ can then be a good measure of this local order at a length scale comparable to the probe size. Thus by measuring the skewness of the distribution of FPT for various lengths of the rod at different temperatures, one would be able to extract ξ_S by performing scaling analysis as shown in Ref. [6] that static length scale controls the finite-size effects of τ_α.

In the top-left panel of Fig. 4, we show the negative of skewness (χ_{FPT}) of the FPT distributions for the 3DKA model while the variation for other models is similar and can be found within the Supplemental Material [9]. The χ_{FPT} is computed as the mean of skewness of 20 consecutive sets of complete data. The standard error computed in this way is smaller than the symbol size. Then scaling by a suitable choice of the length scale $\xi_{rod}^S(T)$ leads to data collapse of skewness versus $L_{rod}/\xi_{rod}^S(T)$ for all temperatures. The data collapse obtained using
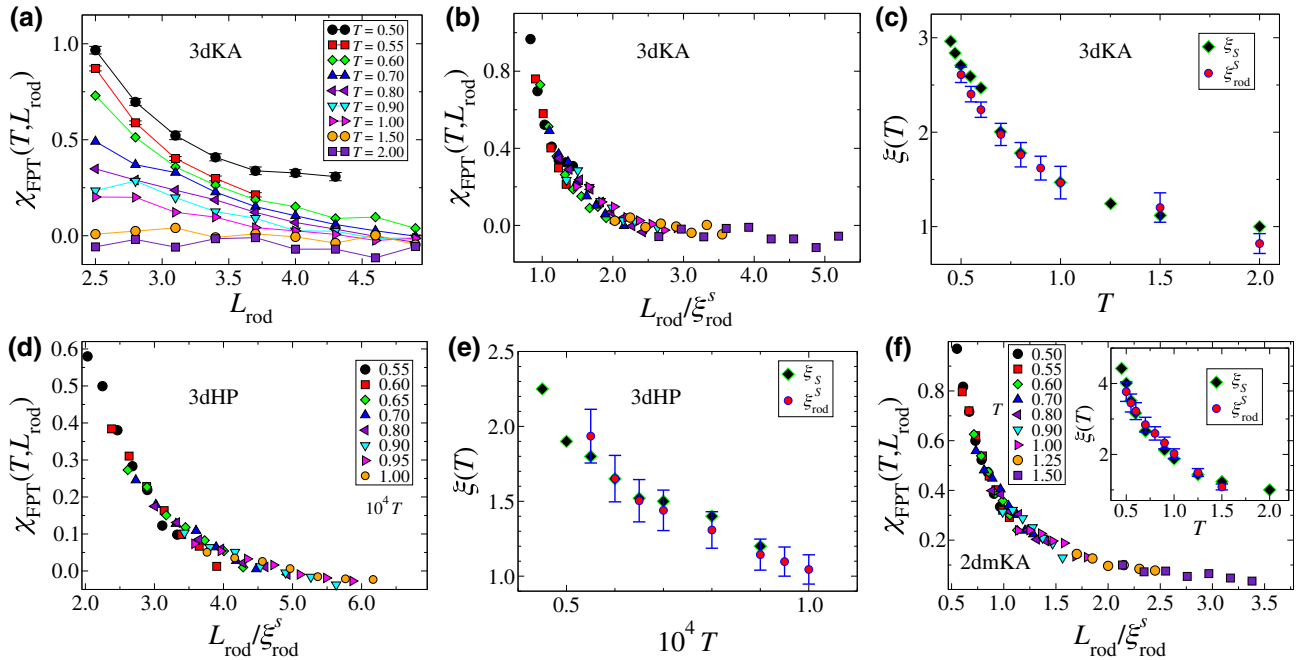

FIG. 4.   (a) Variation in negative of skewness (χ_{FPT}) of distribution, $P[\ln(t)]$ with rod length, where t is the FPT of rod immersed in the 3DKA model liquid at various supercooling temperatures. An increase in skewness with decreasing rod length and increasing supercooling can be clearly seen. (b) The scaling collapse of χ_{FPT} obtained by scaling rod length with appropriate length scale $\xi_{rod}^S(T)$ to obtain a master curve. (d),(f) The similarly obtained collapses for 3DHP and 2DMKA models, respectively. The obtained length scale is plotted and compared with the ξ_S obtained with traditional methods like PTS (3DKA and 2DMKA) and finite-size scaling (FSS) of τ_α using block analysis (3DHP) in (c) (3DKA), (e) (3DHP), and in the inset of (f) (2DMKA).

optimization procedure (see the Supplemental Material [9]) (Fig. 4) for the three model systems are reasonable, and the corresponding length scale is plotted in (c),(e), and in the inset of (f) along with ξ_S obtained using other conventional methods (PTS and block analysis) [24,54]. A near-perfect match of the temperature dependence of $\xi_{\rm rod}^s$ with that of ξ_S suggests that the FPT distribution of the rod indeed captures the static length scale in the system.

V. EXISTING EXPERIMENTAL RESULTS

After understanding the underlying relationship between skewness of the FPT distribution or the rotational relaxation time distribution of the rods with ξ_S of the host supercooled liquid medium, we turn our attention to reanalyze the existing experimental results reported in Ref. [39]. In the left panel of Fig. 5, we show the rescaled distribution of rotation relaxation time, τ of the probe dye molecule in supercooled glycerol, scaled by the time at which the peak appears. The distribution clearly shows that with increasing supercooling, $P[\ln(\tau/\tau_R)]$ starts to show a shoulder similar to simulation results at low temperatures as shown in the right panel of Fig. 5. In the left panel's inset, we show the calculated skewness from experimental data, $\chi_{\rm FPT}$, which seems to decrease very systematically with increasing temperature in complete agreement with our simulation results. This also corroborates the growth of amorphous order in supercooled glycerol, as suggested in Ref. [34]. In the right panel, we show how FPT distribution changes with temperature for a rod length of 2.8 in the 3DKA model. The distributions are scaled by $\tau(T)$, the time when the distribution peak appears at that temperature (see the Supplemental Material [9] for further

discussion). A similar analysis for gold nanorod in supercooled glycerol [42] and dapPDI dye molecule [41] can be found in the Supplemental Material [9]. Although at this moment, we are not able to estimate the growing ξ_S due to lack of experimental data for different length of the probe molecules in supercooled glycerol, we clearly demonstrate the generality and the strength of the proposed methodology for measuring the growth of static correlation in experimentally studied glass-forming liquids.

VI. CONCLUSIONS

To conclude, we show that the rotational dynamics of rodlike probes can be an interesting way to extract the growing static and dynamic correlations in disordered supercooled liquids. We also show analytically that the relaxation-time distribution, although looks similar to log normal, has an entirely different mathematical form. This distribution's statistical properties then allow us to see the supercooling effects. We also verify another vital link between the long observed rotational hopping motion and the liquid structure as proposed in previous theoretical models [43,44]. Our results suggest that to obtain the dynamic heterogeneity and the static length scales quantitatively, one needs to extend the existing experimental studies by systematically changing the length of the probe molecules, which is clearly accessible for experimentally relevant glass-forming liquids.
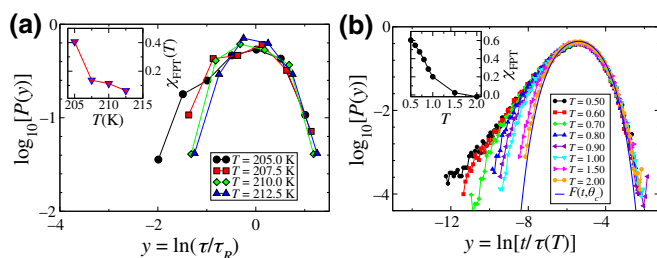
FIG. 5. (a) Distribution of Dye molecules' correlation time in supercooled glycerol for four different temperatures. Data is taken from Ref. [39]. The distribution is rescaled by the mean correlation time. Note the clear signature of a short time shoulder in the distribution at lower temperatures. Inset shows the skewness of the distributions. (b) FPT distribution for a rod of length 2.8 embedded in the 3DKA model for various temperatures. The dashed line through the data points is the best fit to Ref. [8]. The inset shows the skewness of the distribution. The similarity between experimental data and simulation results are very striking.

[1] M. D. Ediger, Spatially heterogeneous dynamics in supercooled liquids, Annu. Rev. Phys. Chem. **51,** 99 (2000), pMID: 11031277.

[2] L. Berthier and G. Biroli, Theoretical perspective on the glass transition and amorphous materials, Rev. Mod. Phys. **83,** 587 (2011).

[3] A. S. Keys, A. R. Abate, S. C. Glotzer, and D. J. Durian, Measurement of growing dynamical length scales and prediction of the jamming transition in a granular material, Nat. Phys. **3,** 260 EP (2007).

[4] T. Kawasaki and H. Tanaka, Structural origin of dynamic heterogeneity in three-dimensional colloidal glass formers

and its link to crystal nucleation, J. Phys.: Condens. Matter **22**, 232102 (2010).

[5] T. Kawasaki, T. Araki, and H. Tanaka, Correlation between Dynamic Heterogeneity and Medium-Range Order in Two-Dimensional Glass-Forming Liquids, Phys. Rev. Lett. **99**, 215701 (2007).

[6] S. Karmakar, C. Dasgupta, and S. Sastry, Growing length and time scales in glass-forming liquids, Proc. Natl. Acad. Sci. **106**, 3675 (2009).

[7] S. Karmakar, C. Dasgupta, and S. Sastry, Growing length scales and their relation to timescales in glass-forming liquids, Annu. Rev. Condens. Matter Phys. **5**, 255 (2014).

[8] S. Karmakar, C. Dasgupta, and S. Sastry, Length scales in glass-forming liquids and related systems: A review, Rep. Prog. Phys. **79**, 016601 (2015).

[9] See Supplemental Material at http://link.aps.org/supple mental/10.1103/PhysRevApplied.16.034022 for definitions, model details, consistency check with different thermostats and barostats, additional results, and a discussion on existing experiments.

[10] T. R. Kirkpatrick, D. Thirumalai, and P. G. Wolynes, Scaling concepts for the dynamics of viscous liquids near an ideal glassy state, Phys. Rev. A **40**, 1045 (1989).

[11] V. Lubchenko and P. G. Wolynes, Theory of structural glasses and supercooled liquids, Annu. Rev. Phys. Chem. **58**, 235 (2007).

[12] G. Biroli, J.-P. Bouchaud, A. Cavagna, T. S. Grigera, and P. Verrocchio, Thermodynamic signature of growing amorphous order in glass-forming liquids, Nat. Phys. **4**, 771 (2008).

[13] G. Biroli, S. Karmakar, and I. Procaccia, Comparison of Static Length Scales Characterizing the Glass Transition, Phys. Rev. Lett. **111**, 165701 (2013).

[14] S. Karmakar, E. Lerner, and I. Procaccia, Direct estimate of the static length-scale accompanying the glass transition, Phys. A: Stat. Mech. Appl. **391**, 1001 (2012).

[15] W. Kob, S. Roldán-Vargas, and L. Berthier, Non-monotonic temperature evolution of dynamic correlations in glass-forming liquids, Nat. Phys. **8**, 164 (2011).

[16] I. Tah, S. Sengupta, S. Sastry, C. Dasgupta, and S. Karmakar, Glass Transition in Supercooled Liquids with Medium-Range Crystalline Order, Phys. Rev. Lett. **121**, 085703 (2018).

[17] R. Das, I. Tah, and S. Karmakar, Possible universal relation between short time β-relaxation and long time α-relaxation in glass-forming liquids, J. Chem. Phys. **149**, 024501 (2018).

[18] L. Berthier, G. Biroli, J.-P. Bouchaud, L. Cipelletti, and W. van Saarloos, eds.*Dynamical Heterogeneities in Glasses, Colloids, and Granular Media* (Oxford University Press, Oxford, 2011).

[19] C. Dasgupta, A. V. Indrani, S. Ramaswamy, and M. K. Phani, Is there a growing correlation length near the glass transition?, Europhysics Letters (EPL) **15**, 307 (1991).

[20] C. Donati, S. C. Glotzer, and P. H. Poole, Growing Spatial Correlations of Particle Displacements in a Simulated Liquid on Cooling toward the Glass Transition, Phys. Rev. Lett. **82**, 5064 (1999).

[21] P. H. Poole, C. Donati, and S. C. Glotzer, Spatial correlations of particle displacements in a glass-forming liquid, Phys. A: Stat. Mech. Appl. **261**, 51 (1998).

[22] I. Tah and S. Karmakar, Signature of dynamical heterogeneity in spatial correlations of particle displacement and its temporal evolution in supercooled liquids, Phys. Rev. Res. **2**, 022067 (2020).

[23] B. P. Bhowmik, I. Tah, and S. Karmakar, Non-gaussianity of the van hove function and dynamic-heterogeneity length scale, Phys. Rev. E **98**, 022122 (2018).

[24] S. Chakrabarty, I. Tah, S. Karmakar, and C. Dasgupta, Block Analysis for the Calculation of Dynamic and Static Length Scales in Glass-Forming Liquids, Phys. Rev. Lett. **119**, 205502 (2017).

[25] E. R. Weeks, Three-dimensional direct imaging of structural relaxation near the colloidal glass transition, Science **287**, 627 (2000).

[26] W. K. Kegel, Direct observation of dynamical heterogeneities in colloidal hard-sphere suspensions, Science **287**, 290 (2000).

[27] Y. Rahmani, K. van der Vaart, B. van Dam, Z. Hu, V. Chikkadi, and P. Schall, Dynamic heterogeneity in hard and soft sphere colloidal glasses, Soft Matter **8**, 4264 (2012).

[28] D. Bonn and W. K. Kegel, Stokes–Einstein relations and the fluctuation-dissipation theorem in a supercooled colloidal fluid, J. Chem. Phys. **118**, 2005 (2003).

[29] C. K. Mishra, A. Rangarajan, and R. Ganapathy, Two-Step Glass Transition Induced by Attractive Interactions in Quasi-Two-Dimensional Suspensions of Ellipsoidal Particles, Phys. Rev. Lett. **110**, 188301 (2013).

[30] L. Berthier, Direct experimental evidence of a growing length scale accompanying the glass transition, Science **310**, 1797 (2005).

[31] L. Berthier, G. Biroli, J.-P. Bouchaud, W. Kob, K. Miyazaki, and D. R. Reichman, Spontaneous and induced dynamic fluctuations in glass formers. i. General results and dependence on ensemble and dynamics, J. Chem. Phys. **126**, 184503 (2007).

[32] L. Berthier, G. Biroli, J.-P. Bouchaud, W. Kob, K. Miyazaki, and D. R. Reichman, Spontaneous and induced dynamic correlations in glass formers. ii. Model calculations and comparison to numerical simulations, J. Chem. Phys. **126**, 184504 (2007).

[33] G. Biroli, J.-P. Bouchaud, K. Miyazaki, and D. R. Reichman, Inhomogeneous Mode-Coupling Theory and Growing Dynamic Length in Supercooled Liquids, Phys. Rev. Lett. **97**, 195701 (2006).

[34] S. Albert, T. Bauer, M. Michl, G. Biroli, J.-P. Bouchaud, A. Loidl, P. Lunkenheimer, R. Tourbot, C. Wiertel-Gasquet, and F. Ladieu, Fifth-order susceptibility unveils growth of thermodynamic amorphous order in glass-formers, Science **352**, 1308 (2016).

[35] K. H. Nagamanasa, S. Gokhale, A. K. Sood, and R. Ganapathy, Direct measurements of growing amorphous order and non-monotonic dynamic correlations in a colloidal glass-former, Nat. Phys. **11**, 403 (2015).

[36] M. T. Cicerone and M. D. Ediger, Relaxation of spatially heterogeneous dynamic domains in supercooled ortho-terphenyl, J. Chem. Phys. **103**, 5684 (1995).

[37] M. T. Cicerone and M. D. Ediger, Enhanced translation of probe molecules in supercooled o-terphenyl: Signature of spatially heterogeneous dynamics?, J. Chem. Phys. **104**, 7210 (1996).

[38] F. R. Blackburn, C.-Y. Wang, and M. D. Ediger, Translational and rotational motion of probes in supercooled 1, 3, 5-tris(naphthyl)benzene, J. Phys. Chem. **100**, 18249 (1996).

[39] R. Zondervan, F. Kulzer, G. C. G. Berkhout, and M. Orrit, Local viscosity of supercooled glycerol near T_g probed by rotational diffusion of ensembles and single dye molecules, Proc. Natl. Acad. Sci. **104**, 12628 (2007).

[40] S. A. Mackowiak, T. K. Herman, and L. J. Kaufman, Spatial and temporal heterogeneity in supercooled glycerol: Evidence from wide field single molecule imaging, J. Chem. Phys. **131**, 244513 (2009).

[41] S. A. Mackowiak, L. M. Leone, and L. J. Kaufman, Probe dependence of spatially heterogeneous dynamics in supercooled glycerol as revealed by single molecule microscopy, Phys. Chem. Chem. Phys. **13**, 1786 (2011).

[42] H. Yuan, S. Khatua, P. Zijlstra, and M. Orrit, Individual gold nanorods report on dynamical heterogeneity in supercooled glycerol, Faraday Discuss. **167**, 515 (2013).

[43] J. Kim and T. Keyes, On the mechanism of reorientational and structural relaxation in supercooled liquids: The role of border dynamics and cooperativity, J. Chem. Phys. **121**, 4237 (2004).

[44] D. Kivelson and S. A. Kivelson, Models of rotational relaxation above the glass transition, J. Chem. Phys. **90**, 4464 (1989).

[45] L. Alessi, L. Andreozzi, M. Faetti, and D. Leporini, Anisotropic jump model of the rotational dynamics in glasses, J. Chem. Phys. **114**, 3631 (2001).

[46] W. Kob and H. C. Andersen, Testing mode-coupling theory for a supercooled binary lennard-jones mixture i: The van hove correlation function, Phys. Rev. E **51**, 4626 (1995).

[47] R. Brüning, D. A. St-Onge, S. Patterson, and W. Kob, Glass transitions in one-, two-, three-, and four-dimensional binary Lennard-Jones systems, J. Phys.: Condens. Matter **21**, 035117 (2008).

[48] C. S. O'Hern, S. A. Langer, A. J. Liu, and S. R. Nagel, Random Packings of Frictionless Particles, Phys. Rev. Lett. **88**, 075507 (2002).

[49] D. C. Rapaport, *The Art of Molecular Dynamics Simulation* (Cambridge University Press, Cambridge, 2004).

[50] M. P. Allen and D. J. Tildesley, *Computer Simulation of Liquids* (Clarendon Press, New York, NY, USA, 1989).

[51] R. Jain and K. L. Sebastian, Diffusing diffusivity: Rotational diffusion in two and three dimensions, J. Chem. Phys. **146**, 214102 (2017).

[52] V. Balakrishnan, *Mathematical Physics* (Springer International Publishing, New Delhi, 2020).

[53] M. Doi, *The Theory of Polymer Dynamics (International Series of Monographs on Physics)* (Oxford University Press, New York, 1988).

[54] R. Das, S. Chakrabarty, and S. Karmakar, Pinning susceptibility: A novel method to study growth of amorphous order in glass-forming liquids, Soft Matter **13**, 6929 (2017).